Pergamon

0301-9322(95)00021-6

Int. J. Multiphase Flow Vol. 21, No. 5, pp. 949–959, 1995

0301-9322/95 $9.50 + 0.00

BRIEF COMMUNICATION

LARGE BUBBLES ATTACHED TO SPARGERS IN DOWNWARDS TWO-PHASE FLOW

R. P. BACON, D. M. SCOTT and R. B. THORPE
Department of Chemical Engineering, Cambridge University, Pembroke Street, Cambridge, CB2 3RA, England

(Received 21 March 1994; in revised form 8 March 1995)

1. INTRODUCTION

This work is concerned with the formation in a downflowing liquid of a gas bubble beneath a gas injector called a sparger. Such bubbles have been observed in an experimental apparatus; the bubbles appear to be attached to the sparger, in the sense that they continue to exist in the presence of fast liquid flows that would cause a free bubble to travel down and out of the pipe. Such bubbles are important in circulating bubble columns used, for example, for a biochemical reaction requiring gas injection in the downcomer to prevent anoxia. The presence of a large bubble is undesirable for two reasons: (1) the available surface area for mass transfer is much less than that for bubbly flow such as that which exists below the bubble, and (2) the density driving force in a circulating bubble column is reduced. This reduction in driving force slows the circulation and possibly stalls the column leading to flow reversal. A full understanding of the bubble would allow prediction of reactor behaviour and the prevention of stalling.

The mechanism which governs the size of the bubble is the entrainment of gas to form small bubbles from the bubble base by the liquid falling down the walls. Previous workers (e.g. Fabre & Line 1992) have commented on the importance of such entrainment in vertical slug flow. Riiser *et al.* (1992) have measured the entrainment rate from the base and the length of a standing Taylor bubble produced in the laboratory. The mechanism for entrainment was examined using high speed photography. Waves moving down the liquid film and shear at the liquid–gas interface combine to draw thin films of gas down from the periphery of the bubble. These thin films then break up into small bubbles in the eddies below the large bubble. Some of these small bubbles rejoin the large bubble and some are drawn down with the flowing liquid.

The similar entrainment of air by plunging liquid jets has been studied in detail by many workers (e.g. van de Sande & Smith 1973, 1976; Kusabiraki *et al.* 1990a, b, 1992; McKeogh & Ervine 1981; Kumagai & Endoh, 1981). Although their results may not apply directly to the present situation it is thought that the general trends reported will apply. Sene (1988) considers planar jets falling down an inclined surface and reports entrainment mechanisms similar to those observed by Riiser *et al.* (1992). The rate at which gas is entrained is a function of the velocity of the falling liquid at the jet base, the size of disturbances on the liquid surface and the physical properties of the liquid. It is expected that these factors will similarly affect the rate of entrainment of gas from the base of a large bubble.

In the case of a large standing bubble in a vertical pipe, the velocity of the liquid at the bubble base, where entrainment occurs, is a function of the liquid flow rate, Q_L. The size of disturbances on the liquid surface at the bubble base is again a function of Q_L (Brauner 1989; Karapantsios *et al.* 1988) and the distance below the nose of the bubble (Takahama & Kato 1980). Obviously, at each stable bubble length, the net rate of entrainment of gas is equal to the rate of supply of gas. Thus, at constant Q_L, each stable bubble length represents the point at which the liquid film is able to entrain gas at the rate at which it is supplied to the sparger. A step increase in air flow rate will cause the bubble to expand downwards. As a result the liquid velocity will increase, the liquid

surface may become more rough and the entrainment rate will increase until it matches the new rate of supply. As the bubble length increases the liquid falls as an annular film on the downcomer walls. When the bubble has grown sufficiently the liquid film will achieve a characteristic film thickness with waves of a characteristic height (Aragaki *et al.* 1987; Karapantsios *et al.* 1989). Any increase in Q_G above the value capable of being entrained by such a film will cause the bubble to expand without bound. This has been observed experimentally and the value of Q_G at which this occurs, will be called the maximum entrainment rate. This maximum entrainment rate is of considerable interest since it is a gas flow rate which corresponds to an infinitely long bubble and, therefore, guarantees that a circulating bubble column must stall.

2. EXPERIMENTAL APPARATUS

The apparatus (see figure 1) consists of a pumped circuit with a vertical, transparent test section approximately 2 m in height and of 5.7 cm internal diameter. Water flow rates were measured using a calibrated orifice plate. A rotameter was used to measure air flow rates and measurements were corrected for air supply pressure. Air flows to the sparger via a needle valve. Q_G was calculated at the pressure of the bubble. Three different sparger designs were used. The first was a horizontal pipe sparger consisting of a horizontal brass pipe, 5 mm i.d., 7 mm o.d., with ten 1 mm air holes arranged in pairs 30° either side of the downwards vertical. The second was a central sparger consisting of a 7 mm o.d. pipe placed in the centre of the liquid flow and tapering to a 2 or 3.4 mm i.d. nozzle. The third was a peripheral sparger consisting of a section of full bore pipe with six 1.4 mm air holes placed uniformly about the circumference and thus injecting air perpendicular to the direction of liquid flow at the tube walls.

Liquid flow rates used were in the range 1.4–3.4 l/s (equivalent to superficial liquid velocities of 0.5–1.3 m/s). Air flow rates used were in the range 1.5–20 l/min (at the pressure in the bubble) which are equivalent to gas superficial velocities of 0.01–0.14 m/s.

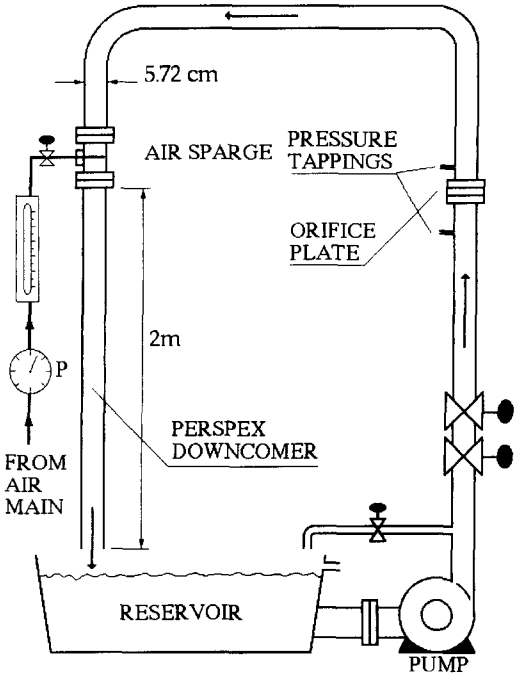

Figure 1. Experimental apparatus.

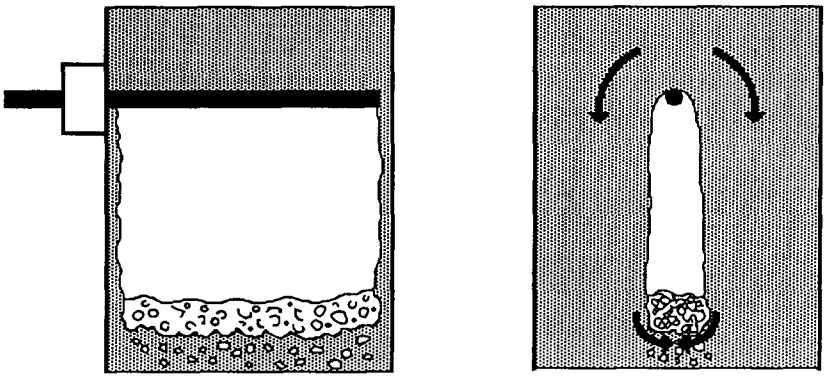

Figure 2. Representation of horizontal sparger bubble at low Q_G/Q_L.

3. INITIAL OBSERVATIONS

The bubble shape has two extremes dependent on both the air and water flow rates. At low ratios of Q_G/Q_L the bubble shape depends upon the design of the sparger. Each sparger design is discussed in turn below.

For the horizontal sparger, at Q_G/Q_L up to about 0.055, the bubble walls are parallel to the length of the sparger. The top of the bubble is attached to the top surface of the sparger at a tangent. The width of the bubble perpendicular to the sparger grows slightly with bubble length (see figure 2). The base of the bubble is a region of high voidage with high circulation from which air is entrained. As the air flow rate is increased the bottom of the bubble moves towards the downcomer

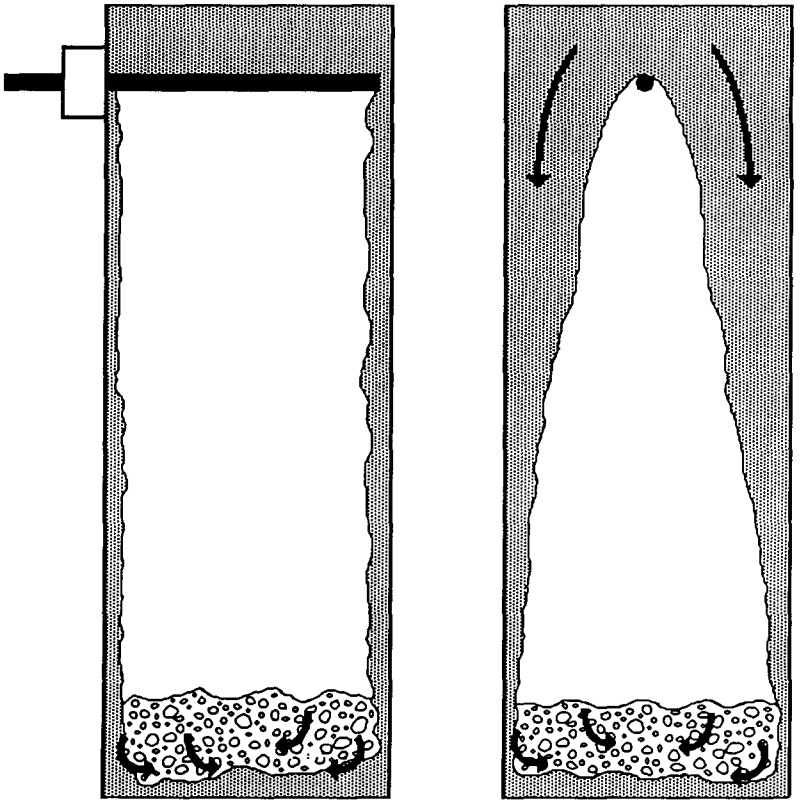

Figure 3. Representation of horizontal sparger bubble at high Q_G/Q_L.

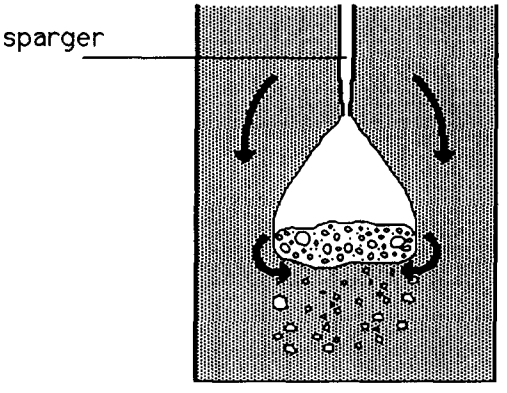

Figure 4. Representation of central sparger bubble at low Q_G/Q_L.

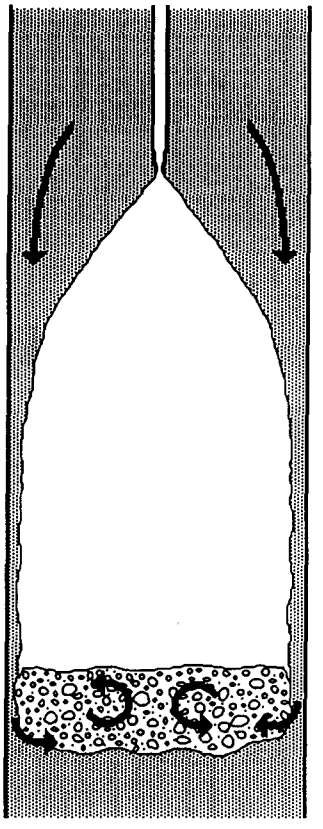

Figure 5. Representation of central sparger bubble at high Q_G/Q_L.

walls. Eventually the base of the bubble becomes cylindrical with the water flowing as an annular film about the bubble (figure 3).

In the case of the central sparger for very low ratios of Q_G/Q_L, particularly for high liquid flow rates, small bubbles are entrained from the nozzle and no large bubble attaches itself to the sparger. At higher Q_G/Q_L the bubble attached to the nozzle grows with a bell shape (figure 4). At the base of the bubble, the surrounding liquid draws air from the bubble into the descending liquid with some re-circulation of small bubbles back to the bubble. As the air flow rate is increased further, the bubble grows towards the tube walls and the water flows down the walls as an annular film (figure 5).

In the case of the peripheral sparger the precise nature of the bubble at low Q_G/Q_L is not clear. Initially, six individual bubbles appear each one attached to an air hole. As the air flow rate is increased these bubbles begin to merge in an approximately random order producing fewer and larger wall bubbles. As the air flow rate is increased further the individual bubbles will all join up to form a ring of air about the downcomer wall. The water now flows down the centre of the tube. This situation is unstable and most of the water finds its way to the downcomer walls with the remainder falling down the centre of the tube (figure 6). Any increase in air flow rate will cause the base of the bubble to grow as a cylinder of air within an annular liquid film flowing down the walls and some water falling freely inside the bubble.

4. STABLE BUBBLE LENGTH, L_s

For a fixed water flow rate, the length of the bubble was measured for a variety of air flow rates. This was repeated for a number of different water flow rates. The experiment was performed with each of the three sparger designs. The results are plotted in figures 7–10. The bubble length increases

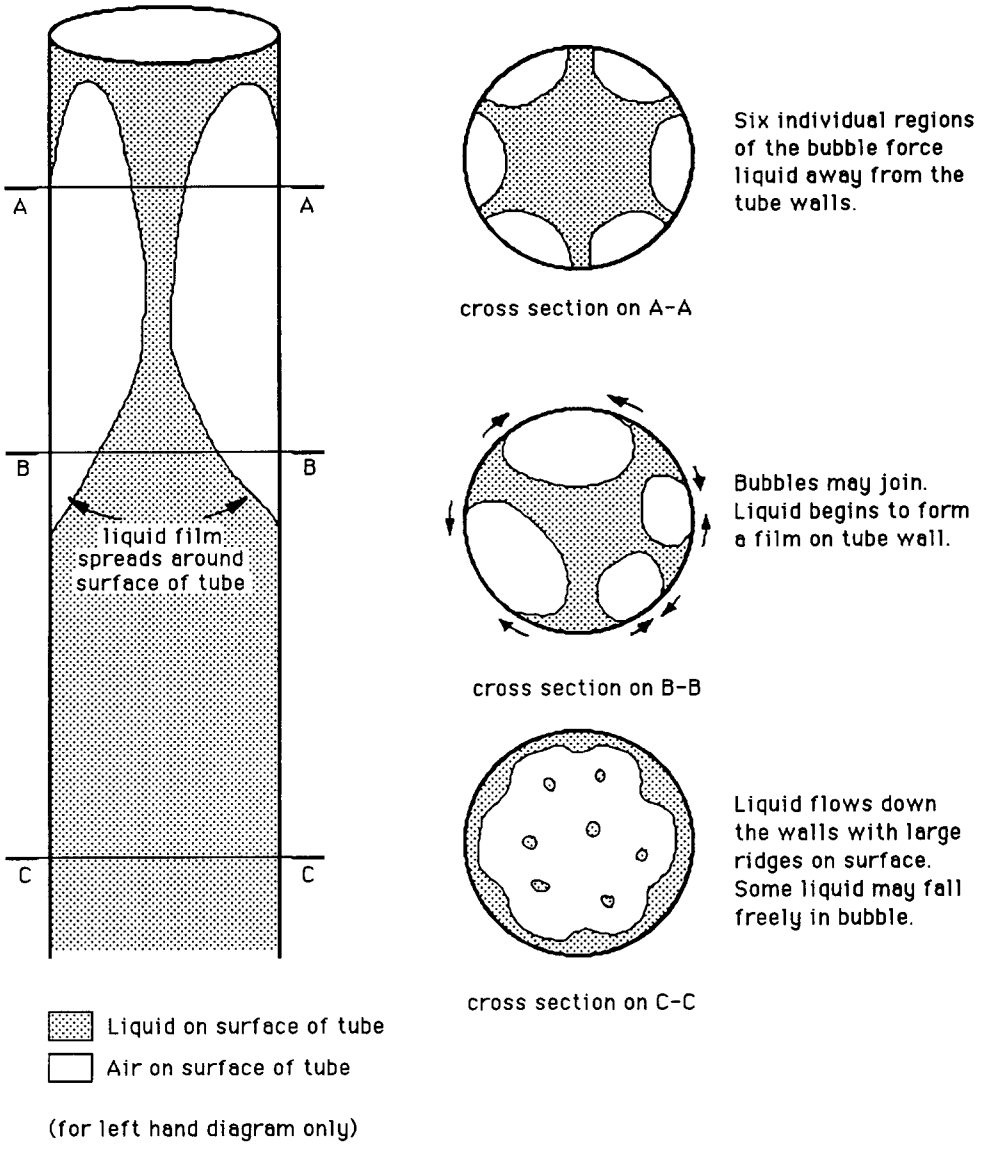

Figure 6. Representation of peripheral sparger bubble at high Q_G/Q_L.

with increasing air flow rate at a given water flow rate and decreases with increasing water flow rate at a given air flow rate. Of the three spargers used, the peripheral sparger produces the shortest bubbles for any combination of air and water flow rates. The central and horizontal spargers both give approximately the same bubble length for a combination of liquid and gas flow rates. The nozzle size for the central sparger has no noticeable effect. At the shorter bubble lengths (the region in which the sparger design has an influence on bubble shape), the horizontal sparger consistently produced shorter bubbles than either of the two central spargers. The difference was of the order of a few centimetres which was slightly larger than the margin of error on the measurements.

For a fixed Q_L the bubble grows as a result of increased Q_G. The resultant increase in bubble length of a unit increase in Q_G increases with bubble length. This is thought to be a result of the annular liquid film surrounding the base of the bubble approaching an equilibrium state in which the film thickness and wave height is constant. As mentioned previously the velocity of the film and the size of the waves upon that film govern the rate of entrainment of air from the bubble. If the bubble is at a stable length and a step change in Q_G occurs while Q_L remained constant, the bubble would expand until the liquid film's properties had changed sufficiently for air to be

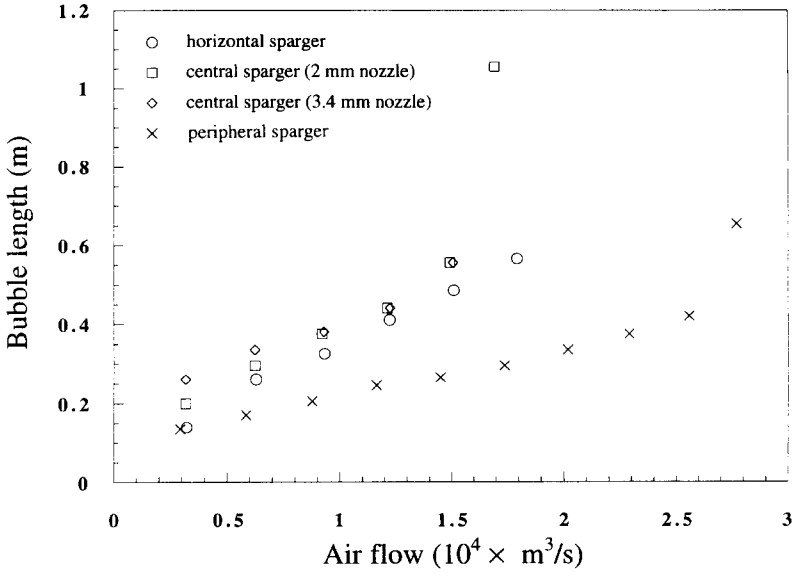

Figure 7. Bubble length vs volumetric air flow rate for $Q_L = 1.34 \times 10^{-3}$ m^3/s.

entrained at the new rate of supply. If the film thickness and wave heights were already fully developed then any increase in Q_G would result in the bubble growing continuously as air supply rate will always be greater than air entrainment rate. In figures 7–10 which show bubble lengths at constant Q_L versus Q_G, the bubble length tends toward infinity at this value of Q_G, the maximum entrainment rate.

5. MAXIMUM ENTRAINMENT RATE, $Q_{G,max}$

To measure the maximum entrainment rate, Q_L was set at a fixed value and Q_G was increased until the bubble grew continuously. The time taken for the base of the bubble to move down a section of the downcomer of known length was recorded. The film thickness for the value of Q_L used was calculated using the method of Dukler & Berglin (1952). The film thickness and the rate

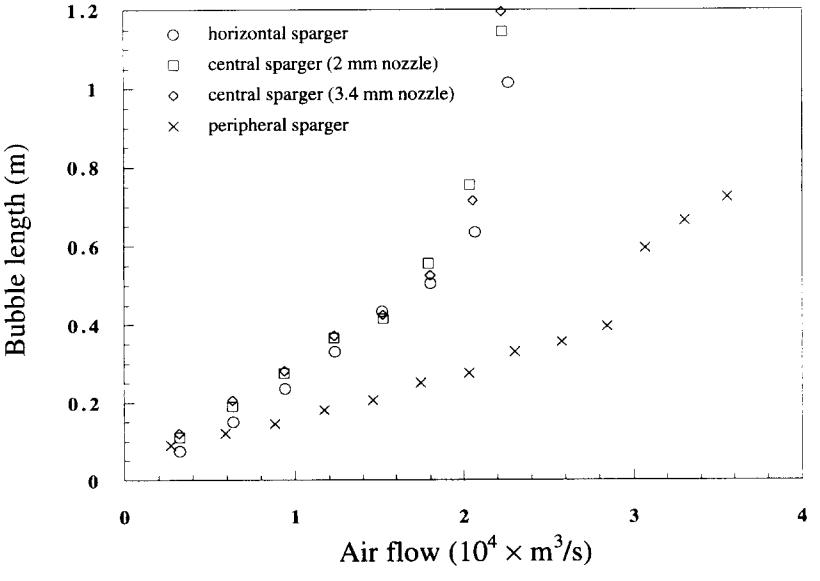

Figure 8. Bubble length vs volumetric air flow rate for $Q_L = 1.81 \times 10^{-3}$ m^3/s.

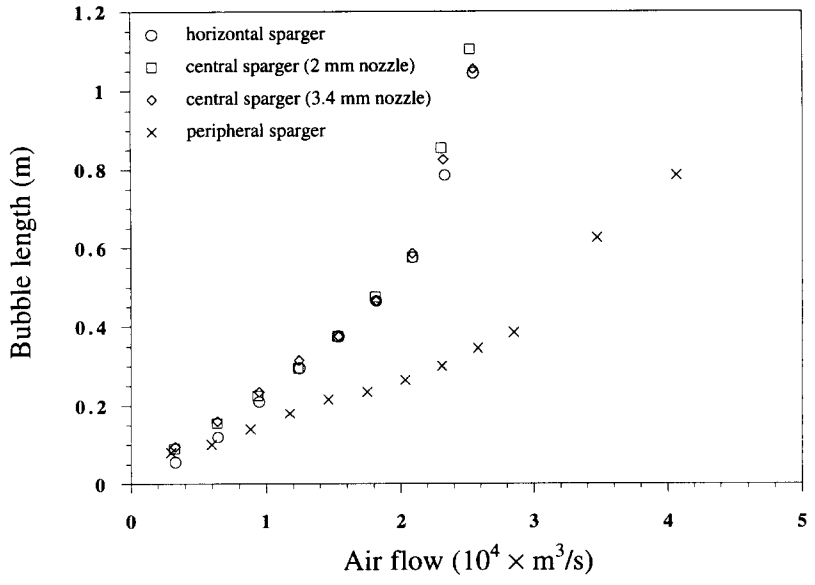

Figure 9. Bubble length vs volumetric air flow rate for $Q_L = 2.12 \times 10^{-3}$ m^3/s.

of increase of bubble length, along with the known internal diameter of the downcomer, were used to find the rate of increase of volume of the bubble. The maximum entrainment rate ($Q_{G,max}$) is the difference between Q_G and this value.

Figure 11 shows the results for each sparger in terms of the parameters suggested by the dimensional analysis presented below. These are the dimensionless maximum entrainment rate, $Fr_{G,max} = Q_{Gmax}/gD^5)^{1/2}$, as a function of a similarly defined dimensionless liquid flow rate, Fr_L. Figures 12 and 13 show the maximum entrainment rate for two of the spargers with a best fit straight line shown. The maximum entrainment rates for the peripheral sparger are significantly larger than those for the other sparger designs. The horizontal and the two central spargers appear to produce essentially the same maximum entrainment rate for a given Q_L. This can be explained by considering the nature of the top of the bubble for each sparger. For the horizontal and central sparger all the water flows smoothly to the downcomer walls and forms a stable film. However,

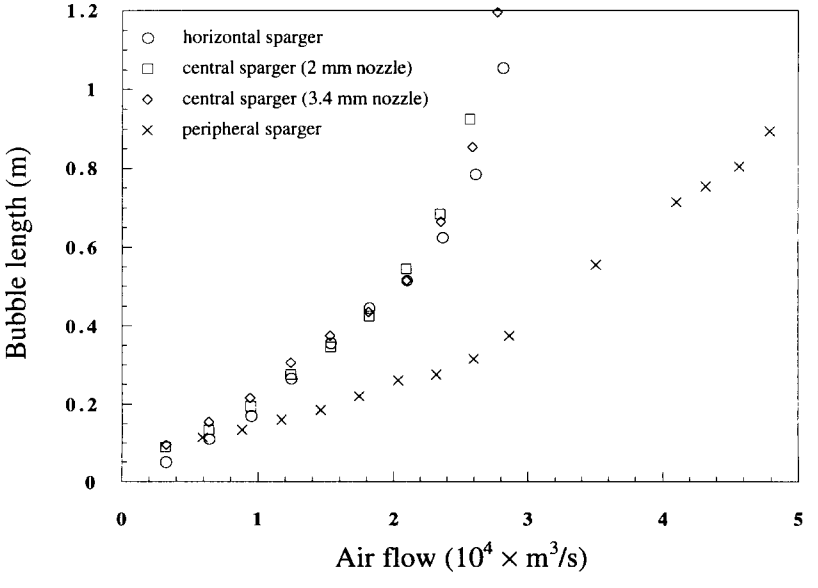

Figure 10. Bubble length vs volumetric air flow rate for $Q_L = 2.35 \times 10^{-3}$ m^3/s.

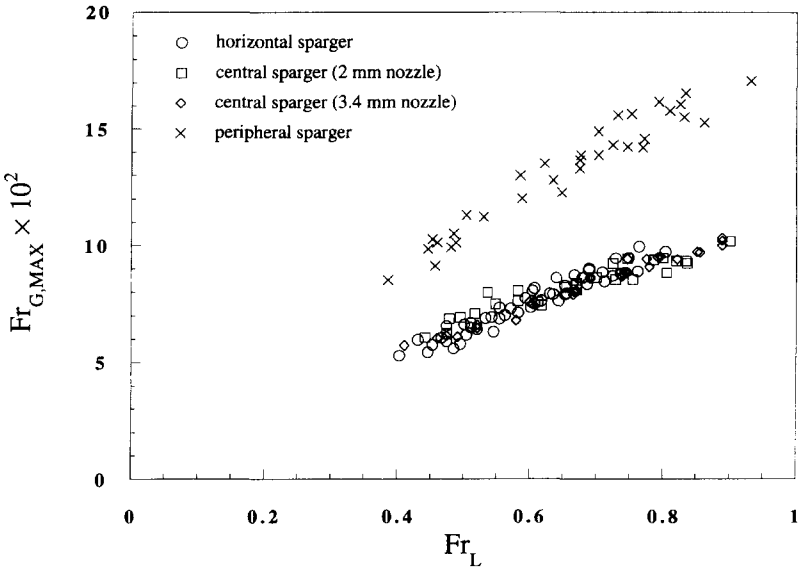

Figure 11. Dimensionless maximum entrainment rates for all spargers.

the flow in the region of the peripheral sparger is somewhat more chaotic or churned and jets and droplets of water fall down the centre of the bubble. There is also a film of water at the wall. There exist vertical "ridges" on this film of significantly larger thickness than the film itself (see figure 6). These ridges correspond to the regions between the air holes in the sparger where the falling water is not pushed away from the wall by a jet of air. These ridges will fall faster than the liquid film as they are thicker than the film. (It is well known that the speed of such a film increases as the film thickness is increased.) It is thought that these ridges increase the entrainment rate significantly. The falling drops of water will also add to the maximum entrainment rate. However, the ridges mentioned above will tend to flatten out as they move down the film, and their contribution to the total entrainment rate will decrease as both size and velocity of the ridges decreases. A critical entrainment rate will now exist. At this point, several factors will combine to cause unbounded bubble growth. The bubble length is such that the ridges on the liquid film are

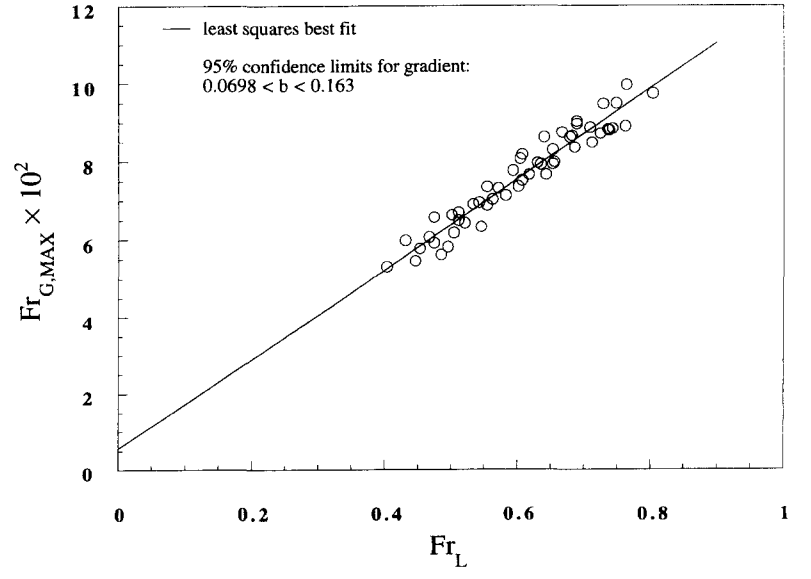

Figure 12. Dimensionless maximum entrainment rates for the horizontal sparger.

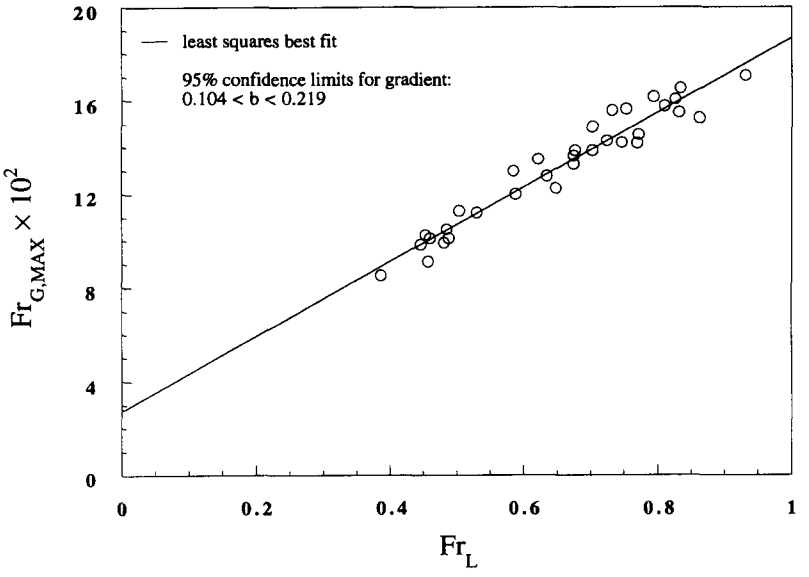

Figure 13. Dimensionless maximum entrainment rates for the peripheral sparger.

flattening out and their contribution to total entrainment rate is decreasing. Film thickness and mean velocity approach an asymptotic value, and hence, this contribution to the total entrainment rate reaches a maximum. Beyond this critical length for the bubble the net entrainment rate decreases and the bubble grows without bound. The air flow rate associated with this bubble length for the given liquid flow rate is the critical entrainment rate.

6. DIMENSIONAL ANALYSIS FOR $Q_{G,max}$

In order to try to predict the behaviour of the bubble in various sized downcomers using different liquid properties a dimensional analysis has been undertaken to determine the groups which affect the bubble.

The rate of air entrainment from the base of the bubble can be written as a function of six variables which, from our knowledge of the behaviour of Taylor bubbles and plunging jets, we expect, apart from the requirement for geometric similarity, to be a sufficient set:

$$Q_{G.max} = \text{function of } \{Q_L, g, \sigma, \mu, \rho, D\}$$

Here g is the acceleration due to gravity, σ is the liquid surface tension, μ is the liquid viscosity and ρ is the liquid density. Therefore, by Buckingham's pi theorem, we require $7-3=4$ dimensionless groups (7 parameters $-$ 3 dimensions). A suitable set is:

$$Q_{Gmax}/(gD^5)^{1/2} = f\{Q_L/(gD^5)^{1/2}, \rho gD^2/\sigma, \mu/\rho(gD^3)^{1/2}\}$$

or

$$Fr_{G.max} = f\{Fr_L, Eö, N_\mu\}$$

where Fr is a Froude number and Eö is an Eötvös number.

The fact that the data shown in figures 11, 12 and 13 lie on straight lines (within experimental error) suggests that it may be possible to simplify the above relation to the following:

$$Fr_{G.max} = [A + BFr_L]$$

where A and B are $f\{Eö, N_\mu\}$ and which also depend on the geometry of the sparger including its dimensions. It will be necessary to conduct experiments in which D, σ and μ are changed in order to test the above hypothesis.

7. DISCUSSION OF SIMILAR WORK

Riiser *et al.* (1992) discuss results of the experiments on entrainment of air from the base of Taylor bubbles. In their experiment, a test section with an annular entry was used to produce a liquid film on the tube wall. Air was injected from the base of the entry section producing a simulation of the base of a Taylor bubble. Measurements of bubble length for various air and water flow rates were made. It was reported that the length of the bubble was linear with varying air flow rate at constant liquid flow rate. Two regions for the rate of increase of bubble length were identified (both linear) with a higher rate of increase at lower air flow rates.

The linear increase in bubble length was confirmed by us at the lower air flow rates used in the experiments reported in this paper. The region of high rate of increase of bubble length was not observed as the low air flow rates used by Riiser *et al.* could not be measured by our rotameter. The liquid flow rates were generally lower than those used by us. We used an open ended downcomer and were therefore restricted in liquid flow rate by the tendency of the apparatus to de-flood (see Thorpe *et al.* 1987, 1989). During de-flooding a large Taylor bubble rises up the wall of the tube from the base causing a transition to annular flow.

We have calculated that the air flow rates used by Riiser *et al.* (1992) were not high enough, at the liquid flow rate used, to approach the maximum entrainment rate. Also, the bubble lengths quoted by Riiser *et al.* were less than half those which correspond to the maximum entrainment rate. We therefore regard our work as complimentary to the work of Riiser *et al.*.

8. CONCLUSIONS

It has been demonstrated that a large bubble forms under spargers in downward vertical two-phase flow. The presence of this bubble will have undesirable effects in many situations. The bubble has been observed to grow with increasing Q_G and decreasing Q_L. In the area where experiments overlap, the rate of increase of bubble length with increasing flow rate was seen to agree with the work of Riiser *et al.* (1992)

A maximum gas entrainment rate for a given liquid flow rate has been identified. This represents an upper limit to the air flow rate which can be used in any such system. It is also a flow rate which must cause a circulating bubble column to stall. This maximum entrainment rate can be increased by the design of the sparger.

Acknowledgements—The authors would like to thank the Science and Engineering Research Council and ICI Bioproducts & Fine Chemicals plc for funding this research project.

REFERENCES

Aragaki, T., Nakayama, S., Suzuki, M. & Toyama, S. 1987 Characteristics of a falling film on a vertical tube. *Int. Chem. Engng* **27,** 326–333.

Brauner, N. 1989 Modeling of wavy flow in turbulent free falling films. *Int. J. Multiphase Flow*, **15,** 505–520.

Dukler, A. E. & Berglin, O. P. 1952 Characteristics of flow in falling liquid films. *Chem. Engng Prog.* **48,** 557–563.

Fabre, J. & Line, A. 1992 Modelling of two phase slug flow. *A. Rev. Fluid Mech.* **24,** 21–47.

Karapantsios, S., Paras, S. V. & Karabelas, A. J. 1989 Statistical characteristics of free falling films at high Reynolds numbers. *Int. J. Multiphase Flow* **15,** 1–21.

Kumagai, M. & Endoh, K. 1982 Effects of kinematic viscosity and surface tension on gas entrainment rate of an impinging liquid jet. *J. Chem. Engng Japan* **15,** 427–433.

Kusabiraki, D., Murota, M., Ohno, S., Yamagiwa, K., Yasuda, M. & Ohkawa, A. 1990a Gas entrainment rate and flow pattern in a plunging liquid jet aeration system using inclined nozzles. *J. Chem. Engng Japan* **23,** 704–710.

Kusabiraki, D., Niki, H., Yamagiwa, K. & Ohkawa, A. 1990b Gas entrainment rate and flow pattern of vertical liquid plunging jets. *Can. J. Chem. Engng* **68,** 893–903.

Kusabiraki, D., Yamagiwa, K., Yasuda, M. & Ohkawa, A. 1992 Gas entrainment behaviour of vertical liquid plunging jets in terms of jet surface length. *Can. J. Chem. Engng* **70,** 181–184.

McKeogh, E. J. & Ervine, D. A. 1981 Air entrainment rate and diffusion pattern of plunging liquid jets. *Chem. Engng Sci.* **36,** 1161–1172.

Riiser, K., Fabre, J. & Suzanne, C. 1992 Gas entrainment at the rear of Taylor bubble. *29th meeting of the European Two-phase Flow Group*, Stockholm, Sweden.

van de Sande, E. & Smith, J. M. 1973 Surface entrainment of air by high velocity water jets. *Chem. Engng Sci.* **28,** 1161–1164.

van de Sande, E. & Smith, J. M. 1976 Jet break-up and air entrainment by low velocity water jets. *Chem. Engng Sci.* **31,** 219–224.

Sene, K. 1988 Air entrainment by plunging jets. *Chem. Engng Sci.* **43,** 2615–2623.

Takahama, H. & Kato, S. 1980 Longitudinal flow characteristics of vertically falling liquid films without concurrent gas flow. *Int. J. Multiphase Flow* **6,** 203–215.

Thorpe, R. B., Moon, R. K., Moore, R. M. & Verghese, T. M. 1987 Two-phase downflow. *3rd Int. Conf. on Multiphase Flow*, The Hague, The Netherlands, Paper K2, pp. 365–381.

Thorpe, R. B., Beresford-Pierse, J. D., Giancola, F. L., McVay, J. & Tabberer, R. J. 1989 Two-phase downflow. *4th Int. Conf. Multiphase Flow*, Nice, France, Paper K4, pp. 397–418.